Wind- and buoyancy-induced transport of the Norwegian Coastal Current in the Barents Sea

Øystein Skagseth,[1,2] Kenneth F. Drinkwater,[1,2] and Emanuele Terrile[3]

Received 28 January 2011; revised 25 April 2011; accepted 11 May 2011; published 4 August 2011.

[1] The focus of this study is on the fluxes and forcing of the Norwegian Coastal Current (NCC) at the entrance to the Barents Sea. The structure and dynamics of the NCC, which consists of a slope branch and an offshore branch, are investigated using (1) a recent 1 year full depth current meter record in the core of the slope region; (2) repeated hydrographic data at an inshore monitoring station; (3) broader regional hydrographic surveys; and (4) atmospheric reanalysis data. The total fluxes are estimated to 1.8 Sv for volume and 26 mSv for freshwater relative to a reference salinity of 34.8, with the largest contributions from baroclinic offshore branch. The heat flux calculated for the slope branch only is 34 TW. These estimates are higher compared to earlier estimates but are based on more comprehensive data. The major mode of variability in the slope branch is consistent with a continental shelf wave on time scales in the range of 3–16 days forced by the along-coast component of the wind stress. Maximum along-slope currents during fall/winter, corresponding to the stronger wind forcing during these seasons, suggest that the observed seasonality in the NCC can be attributed to a similar mechanism.

Citation: Skagseth, Ø., K. F. Drinkwater, and E. Terrile (2011), Wind- and buoyancy-induced transport of the Norwegian Coastal Current in the Barents Sea, *J. Geophys. Res.*, *116*, C08007, doi:10.1029/2011JC006996.

1. Introduction

[2] The Norwegian Coastal Current (NCC) is important in a climate context because it transports heat and low-salinity water northward, that eventually maintain the cold Arctic halocline [*Aagaard et al.*, 1981]. Numerous studies have also related properties of the NCC to the fisheries. *Helland-Hansen and Nansen* [1909] showed that the catches of sprat (*Sprattus sprattus*) varied in phase with temperature on the west coast of Norway. *Eggvin* [1940] investigated the effect of the cold water front off the west coast of Norway on the herring (*Clupea harengus*) fishery. Later, *Eggvin* [1946] connected the spawning site of the northeast Arctic cod (*Gadus morhua*) in the Lofoten area to the depth of the transition layer between the NCC and the underlying Atlantic Water. The importance of the NCC flowing over banks in generating retention areas for fish eggs and larvae has been suggested by *Sætre* [1999], and the drift of herring and cod larvae northward with the NCC (and the offshore Norwegian Atlantic Current) are highly sensitive to the wind forcing and hydrographic conditions [*Vikebø et al.*, 2005].

[3] The NCC is a buoyancy-driven coastally trapped current [*Garvine*, 1995] carrying low-salinity water along the Norwegian coast and into the Barents Sea (Figure 1) [*Hjort and Gran*, 1899]. The freshwater input at the origin, here defined at the Baltic entrance to the Skagerrak, is about 15,000 m^3 s^{-1} with the major contribution from the Baltic Sea outflow [*Knudsen*, 1899] and a minor contribution by North Sea river runoff [*Baliño*, 1993]. As the NCC flows along the Norwegian coast it receives additional local freshwater discharge, at an annual rate of 12,000 m^3 s^{-1} [*Tollan*, 1976]. Despite this latter contribution, the upper layer salinity increases northward and the lower-layer salinity decreases, due to mixing with the ambient offshore Atlantic water, thus producing a more uniform vertical distribution to the north [*Helland-Hansen and Nansen*, 1909].

[4] Through the year there are substantial variations in the hydrographic conditions in the NCC. Beginning in fall and through the winter, cyclones cause southwesterly winds, which produce downwelling-favorable conditions along the coast. During spring and summer the cyclonic winds are reduced and upwelling-favorable winds become more frequent [*Iden*, 1997]. This effect was noted by *Helland-Hansen and Nansen* [1909] who reported wind-induced seasonal lateral displacement of the coastal waters. This results in the wedge-shaped coastal waters being deep and narrow during winter and wide and thin during summer [*Sætre*, 2007].

[5] The seasonality of the discharge differs from that of the wind. The maximum Baltic outflow is observed during January–February [*Gustafsson*, 1997] while the maximum discharge from Norwegian Rivers is in May–June, associated with the snowmelt [*Tollan*, 1976]. The interplay between the wind and the buoyancy forcing varies through the year. *Whitney and Garvine* [2005] defined a wind

[1]Institute of Marine Research, Bergen, Norway.
[2]Bjerknes Centre for Climate Research, University of Bergen, Bergen, Norway.
[3]Data Environment Analysis Modelling, Pisa, Italy.

0148-0227/11/2011JC006996

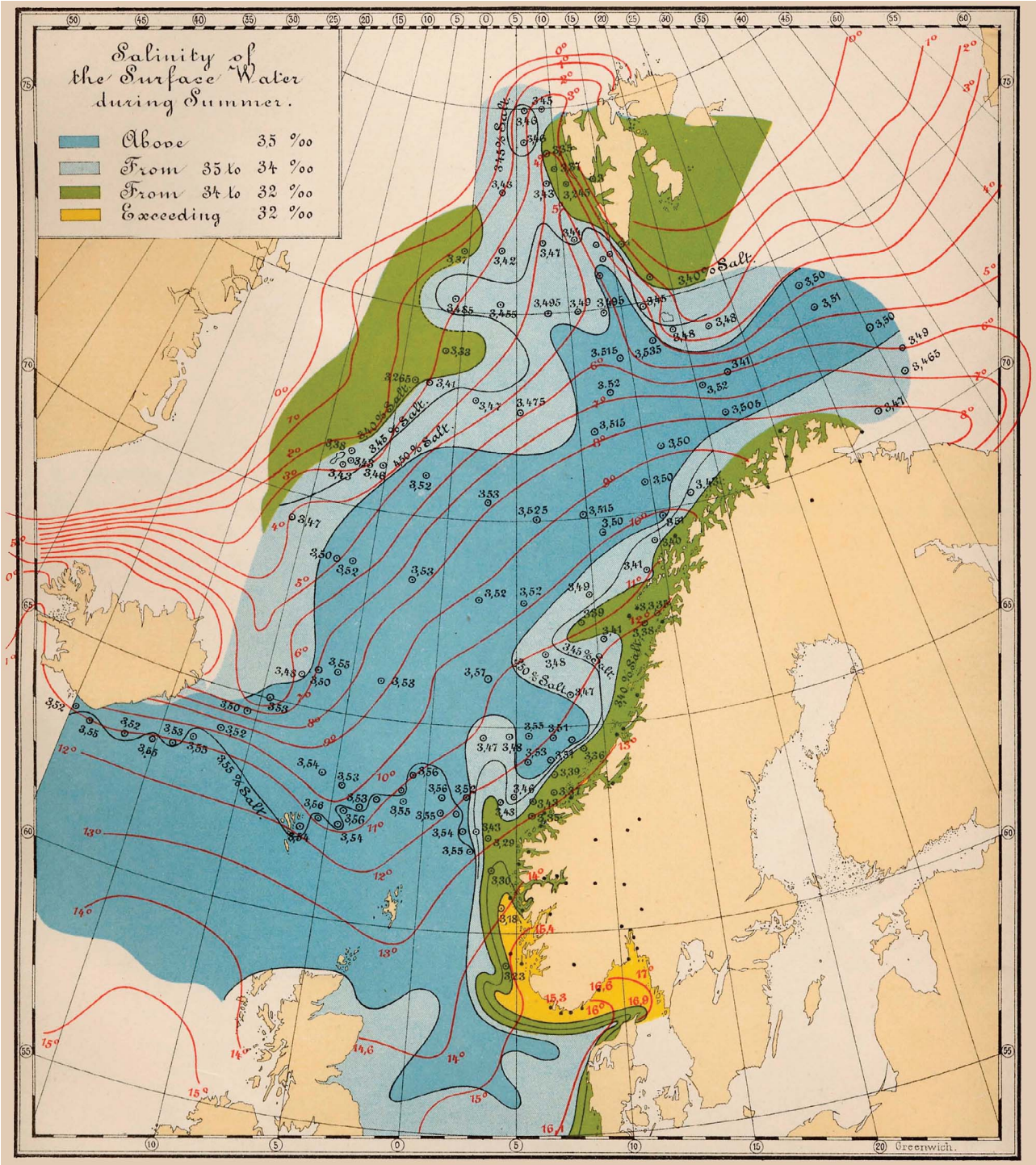

Figure 1. Composite temperature and salinity distribution based on observations from *Hjort and Gran* [1899].

strength index that determines whether a freshwater plume's along-shelf flow is wind or buoyancy driven. This index depends on the strength of the along-coast wind stress, the reduced gravity determined by the density of the NCC waters and the ambient Atlantic Water, and the freshwater discharge rate. As these properties vary along the coast, the index and thus the importance of the wind relative to the buoyancy forcing in driving the NCC is also expected to change.

[6] Previous studies have mostly focused on the NCC northward to the Tromsøflaket region (Figure 2) [*Sætre and Mork*, 1981]. Here the density contrast between the coast water and the ambient AW is relatively large and the NCC is principally density driven [*Garvine*, 1995]. On short time scales (of order days) there is a strong effect of traveling

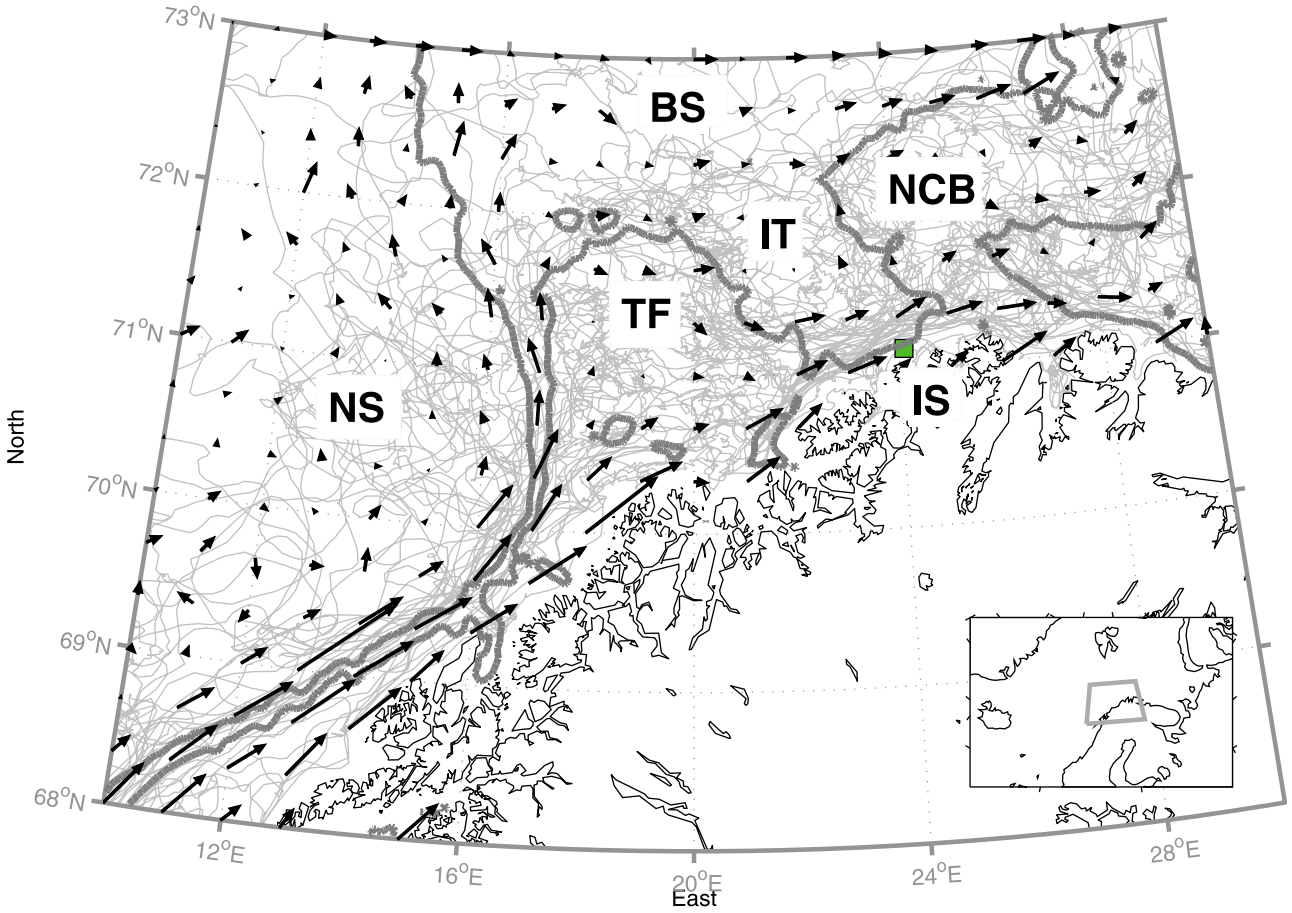

Figure 2. Trajectories from subsurface drogued drifters crossing the Ingøy section between 70.8°N and 71.6 N° (total of 41). The arrows represent the mean drifter velocities from boxes of 1/3° latitude by 1° longitude. Data are from the NODC. The abbreviations are as follows: NS, Norwegian Sea; BS, Barents Sea; TF, Tromsøflaket; NCB, North Cape bank; IT, Ingøy Trough; IS, Ingøy fixed hydrographic station.

cyclones along the west coast of Norway [*Martinsen*, 1981] that can force continental shelf waves [*Gill*, 1982]. However, since the density contrast between the Coastal Water and the Atlantic Water is reduced northward, one might hypothesize that the wind becomes relatively more important as driver of the NCC in the Barents Sea.

[7] The focus of this paper is on the NCC at the entrance to the Barents Sea. Based on near surface drogued drifters, the pathways of the NCC is complex in the region of Tromsøflaket before converging toward the continental slope near Ingøy (Figure 2). Here the simple topography consisting of a narrow continental shelf, a continental slope of width 15 km, followed by the relative flat bottom of the Ingøy depth of ~350 m, makes this an ideal location for monitoring. A recently obtained 1 year full depth current meter record off Ingoy, in combination with repeated hydrographic profiles, provides the possibility to investigate the role of the buoyancy and the wind forcing in this region, and the associated fluxes of volume, heat and freshwater. The most cited NCC volume flux estimate [*Blindheim*, 1989] of 0.8 Sv is based on a 1 month record only, and the baroclinic transport in the entrance to the Barents Sea is 0.7 Sv [*Björk et al.*, 2001]. These estimates correspond well, but as will be shown, the total volume flux of the NCC exceeds these values by a factor of more than two.

2. Data

[8] The current profile data were from a bottom-mounted upward looking acoustic Doppler current profiler (ADCP) in a trawl-proof frame. The ADCP was a RDI Workhorse Long Ranger. The manufacturer provided an accuracy of 1% or 0.005 ms^{-1} for the velocity measurements and the compass was good to ±2°. The beam angle was 20° and beam width as 4°, while the ping rate was set to 1 Hz. The instrument was moored at the bottom in about 204 m of water. The vertical cell size was set to 8 m and the averaging period to 20 min. The first good bin was at 188 m depth, then at 8 m intervals up to 24 m depth. Closer to the surface the data become noisy, partly due to the spherical effect of the ADCP sound pulse, and have been discarded from the analysis. The instrument was deployed from 2 July 2007 to 16 July 2008 at 71°08.02′N and 24°00.96′E. The tidal currents were significant at all depths but not a focus of this study. A Hamming window [*Oppenheim and Schafer*, 1989] of length 40 h was applied to the ADCP data to remove variability at time scales ≤1 day.

[9] Hydrographic data were taken from two different sources that combined provided information on both the long-term temporal changes and the spatial variability. The long-term hydrographic variability was obtained using the repeated hydrographic station at Ingøy just north of the ADCP mooring position in 300 m depth. This station was initiated by Jens Eggvin in 1935 as part of the coastal climate monitoring [*Aure and Østensen*, 1993; *Sætre et al.*, 2003]. New profiles have been obtained 1–2 times per month, giving 1386 profiles by the end 2008. The spatial hydrographic variability was captured by gridding hydrographic data from various surveys from 2000 to 2007 and includes a total of 725 stations. These data allow resolution of the spatial hydrographic variability on a seasonal scale.

[10] Daily surface wind stresses were obtained from the ECMWF ERA Interim data set (http://data-portal.ecmwf.int/data/d/interim_daily/) given at 1.5° latitude by 1.5° longitude spatial resolution.

3. Current and Hydrographic Variability

[11] The trajectories of near-surface drogued drifters suggest that the flow is a topographically steered current in the vicinity of the Ingøy section (Figure 2). Both upstream, over the Tromsøflaket, and downstream, toward the North Cape Bank, the flow field appears to be more chaotic (Figure 2).

[12] The horizontal salinity field at 25 m shows the influence of the fresher coastal water close to the coast that becomes more saline farther seaward due to a larger fraction of Atlantic Water (Figure 3). A similar pattern is found at the 100 m depth but with higher salinities. Note that the isohalines upstream of the North Cape Bank are aligned more parallel to the coast at the 25 m compared to 100 m depth. Vertical slices of the hydrography in the Ingøy section show clear seasonal differences. During winter (DJF) (Figure 4) the fresh NCC extends relatively deep and is confined within less than 100 km of the coast, and further offshore followed by a region with vertically homogeneous water. In contrast the NCC is much shallower during summer (JAS), extends much further from the coast, and the density is vertically stratified throughout the section (Figure 5).

[13] The vertical current profile from the ADCP shows remarkably stable current orientation, being aligned roughly along the isobaths throughout the water column (Figure 6). Only at the lowermost depth cell (188 m) is there an indication of a significant cross-isobath component, which is consistent with a bottom Ekman layer. The upper layer (28–44 m) mean velocity of 0.34 m s^{-1} is reduced to 0.11 m s^{-1} near bottom (172–188 m; see Table 1 for details). Divided into seasonal means (Table 1), the velocities are at maximum in the fall/winter, with upper layer velocities decreasing by approximately 0.10 m s^{-1} during spring/summer. The vertical shear is typically larger during fall/winter compared to the spring/summer seasons. This is in accordance with larger horizontal salinity (and density) gradients due to a narrower and deeper NCC during winter compared to summer (compare Figures 4 and 5).

[14] On periods longer than 1 day, there is a large degree of covariability throughout the water column but the amplitudes decrease with depth (Figure 7). The most pronounced events occur during the winter and show a barotropic response to atmospheric forcing. To elaborate on the spatiotemporal variability, a real vector empirical function analysis [*Kaihatu et al.*, 1998] was applied to the current meter data (Figure 8). The leading empirical orthogonal function (EOF) mode, representing 84% of the variability, has a spatial structure that resembles the mean velocity profile (Figure 8a), i.e., oriented along the isobaths. The associated principal component to the leading EOF mode shows variability over a broad range of scales. The seasonal variability of the NCC is captured by this mode, in accordance with the seasonal variability presented in Table 1. As revealed by the stick plot (Figure 7), the most pronounced events occur during fall and winter, whereas the period from July to September appears quiet (Figure 8b).

[15] The large variance captured in the leading EOF mode warrants further analysis of its temporal evolution (PC1, Figure 8b). There is a significant relation between the variability of the PC1 and the local along-coast wind (ACW) at Ingøy for time scales from 3 to 16 days (Figure 9, top), with a phase lag such that the current variability lags the local ACW variability (Figure 9, middle). In our case of both varying stratification and topography, the response is expected to be in terms of a continental trapped wave (CTW), a class of hybrid wave that is a combination of internal Kelvin waves and barotropic continental shelf waves [*Gill and Clarke*, 1974]. These two classes of waves obey the similar generic equation. Therefore to investigate the combined effect of both local and nonlocal forcing, a CTW model [e.g., *Gill*, 1982; equation 10.12.25] can be applied

$$\frac{1}{c_n}\left(\frac{\partial V_n}{\partial t}+r_n V_n\right)+\frac{\partial V_n}{\partial y}=\frac{b_n Y_S(y,t)}{\rho\, f}, \qquad (1)$$

where c_n is the speed of the propagating wave, r_n^{-1} is the decay time scale, and b_n is the effect of the wind forcing, y is an axis system defined along the coast and Y_s is the along-coast component of the wind stress, ρ is the density of seawater, and f is the Coriolis parameter. The model coefficients depend on the shelf topography that, typically as well as along the Norwegian shelf, varies both in width and depth. Therefore, one cannot expect one set of parameters that applies to all locations along the coast. The approach here is to seek a parameter set to *minimize the phase difference* between the model (equation 1) and PC1, the latter representing the main temporal variability of the current meter data. Solutions are sought in the ranges of propagation speed (c_n) from [1–7] m s^{-1} and decay time scale (r_n^{-1}) of [1–7] days. The parameter set that gives the best fit to the current meter data is for c_n = 2.5 m s^{-1} and r_n^{-1} = 4.5 days. The wind efficiency parameter b_n = 10^{-6} m^{-2} does not affect the coherence analysis and is chosen in order to match the variance of the CTW model and the current meter data. The existence of a set of coefficients within a reasonable (previously published) range that improve the coherence using the CTW model indicates that the CTW is an important mode of variability. Also, the relative good fit to the local along-coast wind (Figure 9, bottom) indicates the rather high degree of covariability of the wind field along the coast (Figure 10).

4. Transports by the Norwegian Coastal Current

[16] Flux estimates of heat and salt depend on the choice of a reference value for sections where an area of a net zero

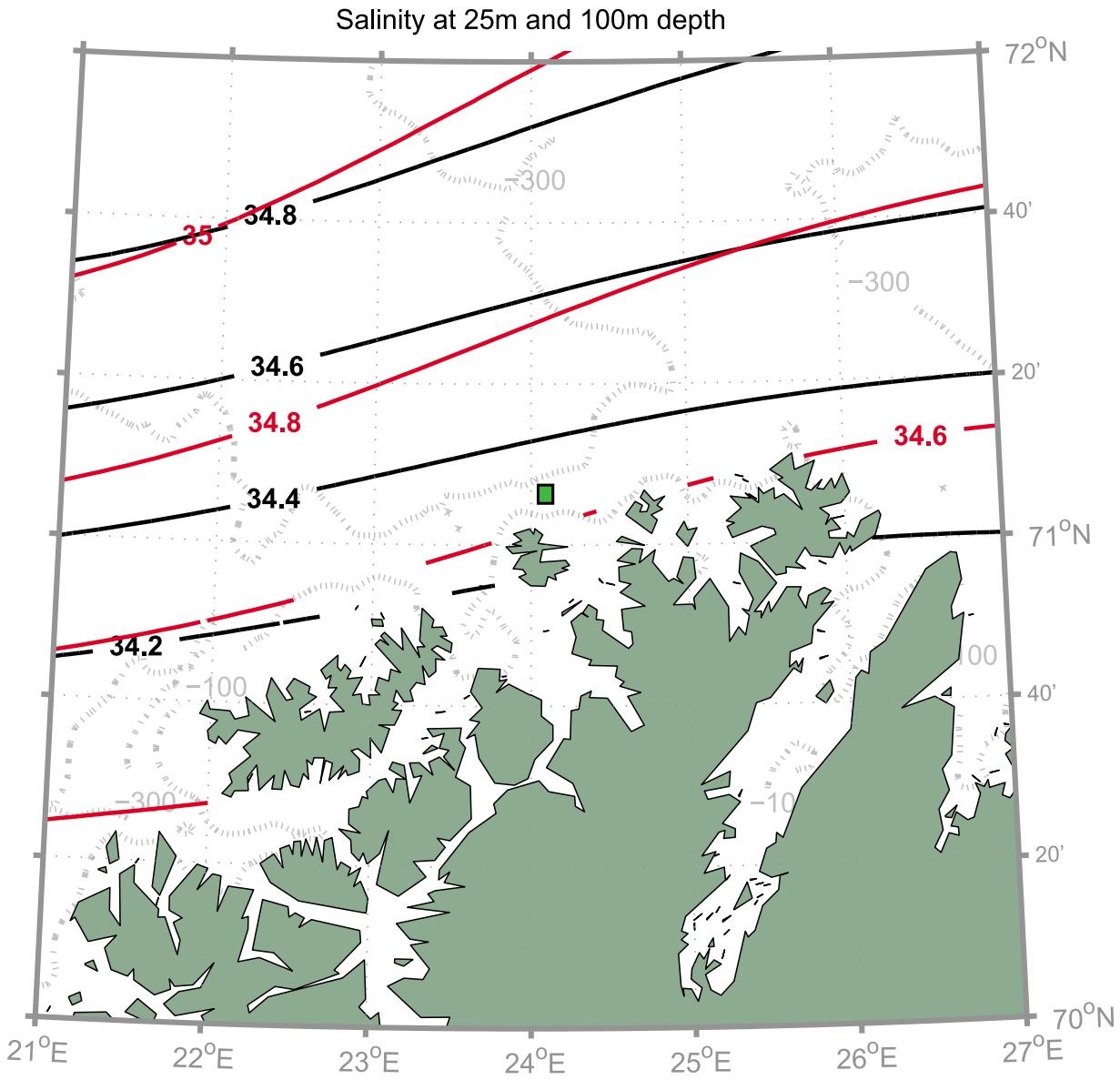

Figure 3. Horizontal plots of salinity at 25 (black) and 100 m (red). The 100 and 300 m isobaths are included (gray dotted lines). This is based on 725 hydrographic profiles obtained from the years 2000 to 2007. The data are most frequent during spring and fall. The successive correction method [*Bratseth*, 1986], a method related to optimal interpolation, is used to plot the data. The mooring site is shown by a green square.

volume flux cannot be achieved [*Montgomery*, 1974; *Schauer et al.*, 2008]. In this study we rely on the traditional approach of using reference values linked to the upstream source, or downstream sink [e.g., *Dickson et al.*, 2007]. Whether this is fundamentally correct can be argued, but it provides the possibility to compare with other sources, and previous estimates. For the heat flux we use a reference T of 0°C that is close to the mean outflow temperature to the Arctic in the Northeast Atlantic. For the freshwater flux we use two reference values; 34.8 to conform with the majority of reported estimates in the literature [*Dickson et al.*, 2007] and 35.0 that is close to the mean salinity of the Atlantic water in the Barents Sea Opening and used in a box model of the Barents Sea [*Smedsrud et al.*, 2010].

[17] The simple topography at the Ingøy section consists of a very narrow (~1–2 km) and shallow (25 m) shelf, a slope region, and an offshore region of 350 m depth, which allows separation of the different contributions to the transports (Figure 11). In the following, the shelf is not considered since its contribution to the fluxes probably is negligible due to its small width and depth, plus it would be difficult to quantify. However, the two major contributions to the transports, the slope and the offshore region, can be treated separately. Such a separation of the branches was previously found for the Norwegian Atlantic Current [*Orvik*

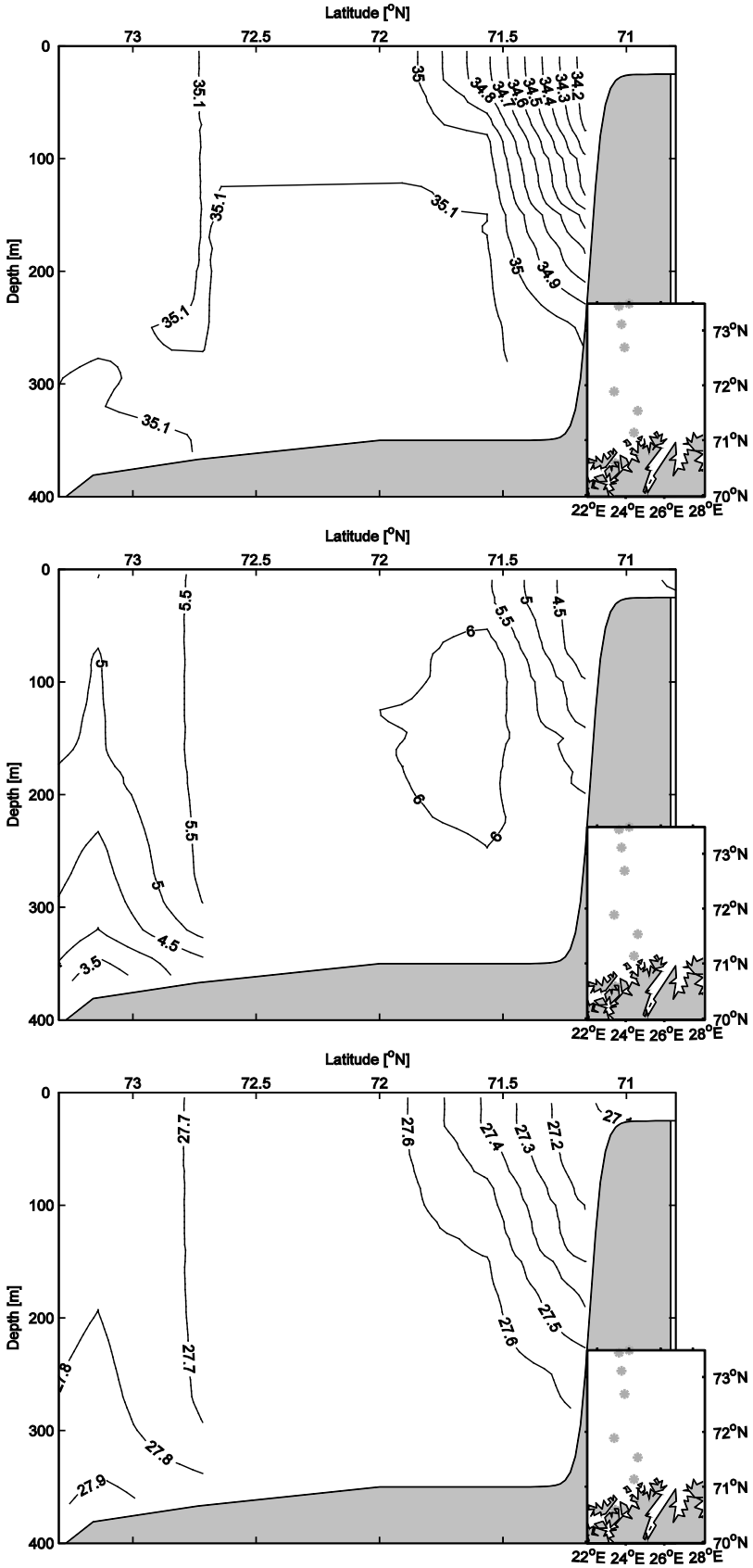

Figure 4. Cross section normal to the coast at Ingøy showing (top) salinity, (middle) potential temperature, and (bottom) potential density relative to the surface. The plots are obtained using all stations obtained along the Ingøy section (see lower right) obtained during the winter (DJF) of 2007–2008.

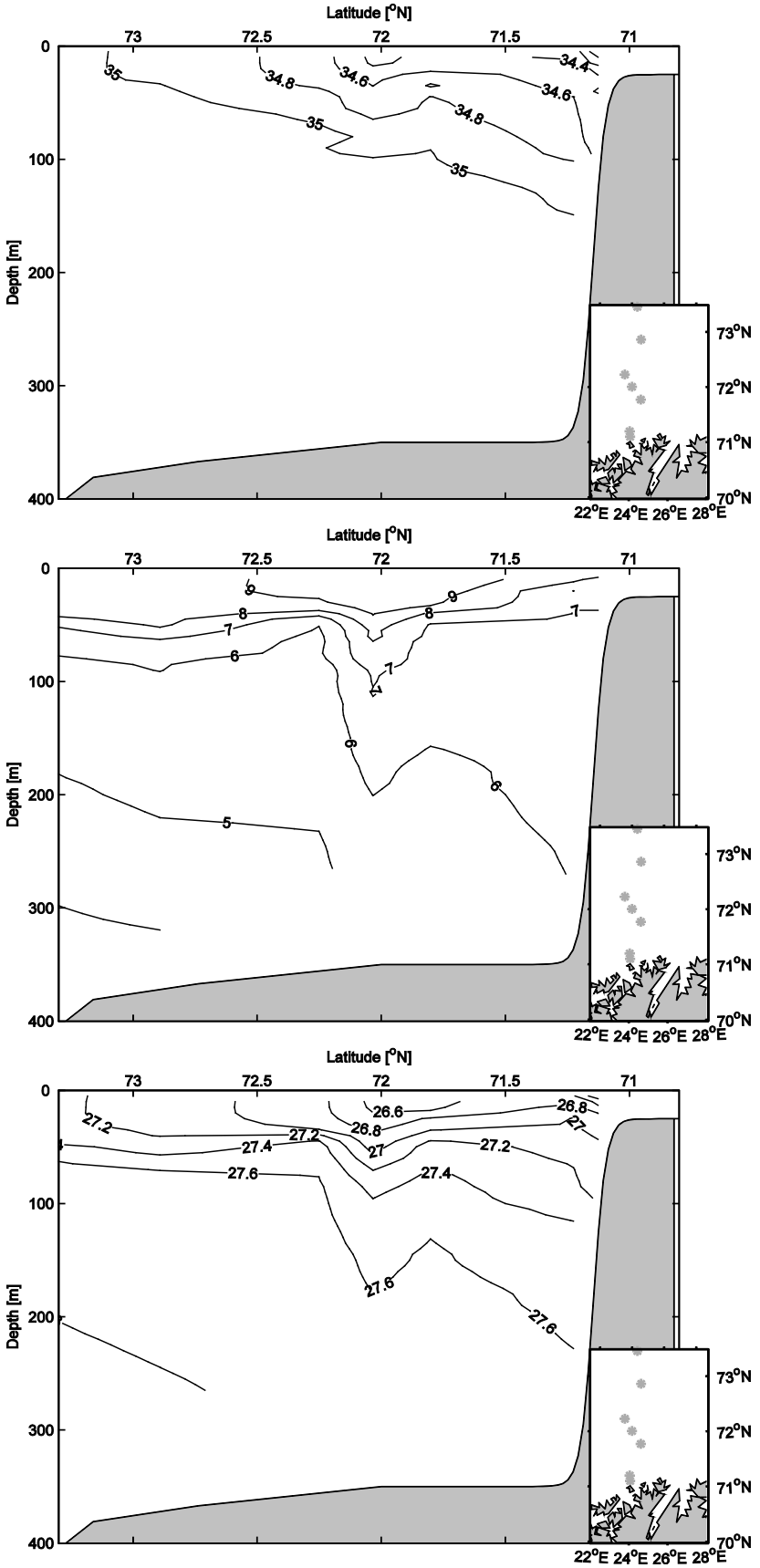

Figure 5. The plot is similar to as in Figure 4 but showing summer conditions. All stations obtained along the Ingøy section (see lower right) obtained during summer (JAS) of 2007 are used.

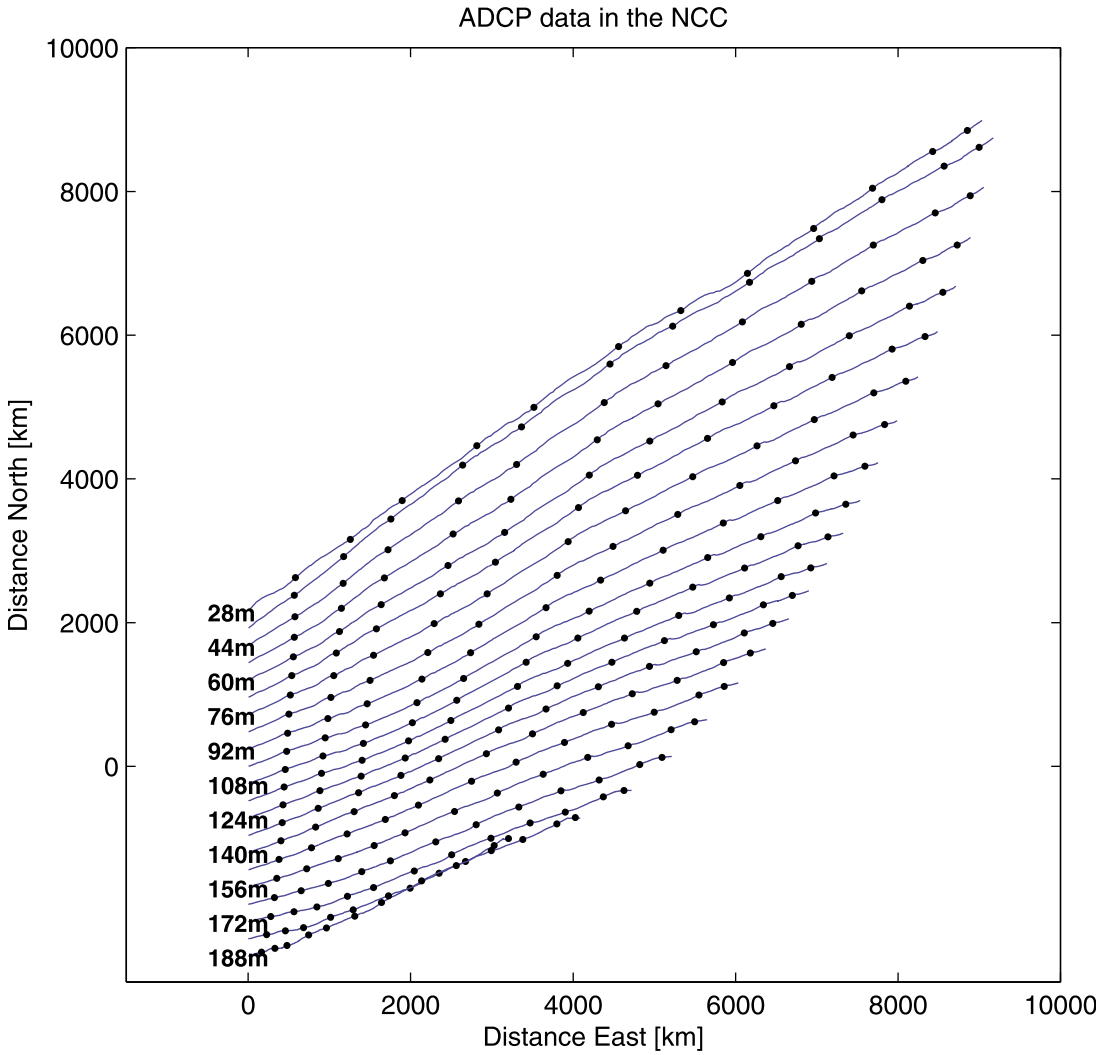

Figure 6. Progressive vector diagram for the ADCP current meter data. Current records representing various depths are shifted vertically for illustration purposes. Period is 2 July 2007 to 16 July 2008. Data are filtered using a Hamming window of length 40 h. The bullet points starting 1 August indicate the start of a new month.

et al., 2001]. Finally, according to the theory of *Walin et al.* [2004] the contribution from the baroclinic branch should transfer into the slope branch in proportion to buoyancy loss.

[18] The first contribution comes from the slope region where a crude estimate of the velocity field can be inferred based on the current profiler located at middepth and the hydrographic data.

[19] Starting from the conservation of potential vorticity

$$\frac{D}{dt}\left(\frac{f+\eta}{H+\zeta}\right) = 0, \tag{2}$$

where f and η are the Coriolis parameter and the relative vorticity, respectively, and H and ζ are the bottom depth and the sea surface elevation, respectively. Assuming stationary

Table 1. Mean Values and Seasonality for Currents at Upper, Intermediate, and Lower Depths Based on the ADCP Data[a]

	Mean		Winter (JFM)		Spring (AMJ)		Summer (JAS)		Fall (OND)	
Depth (m)	V (cm s^{-1})	Direction (°)	V (cm s^{-1})	Direction (°)	V (cm s^{-1})	Direction (°)	V (cm s^{-1})	Direction (°)	V (cm s^{-1})	Direction (°)
28–44	34.1	35	38.9	33	29.1	31	27.0	38	42.2	38
ΔV	9		9		6		8		14	
92–108	25.0	25	29.3	27	23.0	23	19.4	21	28.9	29
ΔV	14		14		11		13		17	
172–188	11.1	27	15.2	30	12.4	29	6.6	15	11.7	26

[a]The upper, intermediate, and lower depths are 28–44, 92–104, and 172–188 m. The intermediate rows give the vertical shear.

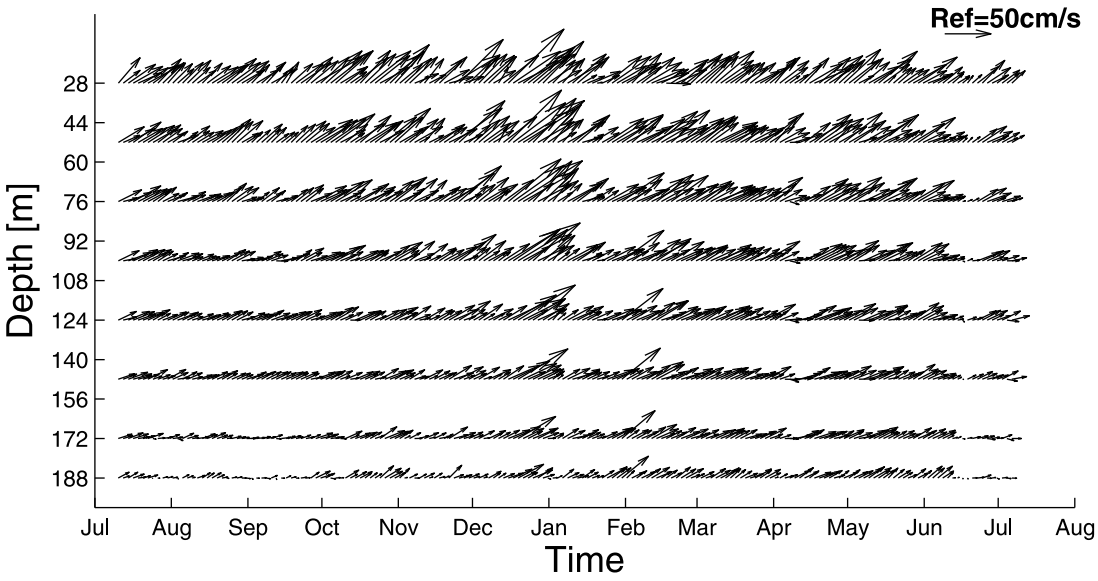

Figure 7. Stick plot for the ADCP current meter data. Current records that represent various depths are shifted vertically for illustration purposes. Period is 2 July 2007 to 16 July 2008. Data are filtered using a Hamming window of length 40 h.

conditions, $|\eta| \ll$ fand $|\zeta| \ll H$, and that $|\nabla\zeta| \ll |\nabla H|$ and $H|\nabla\eta| \ll f|\nabla H|$ this reduces to

$$\vec{v} \bullet \nabla\left(\frac{f}{H}\right) = 0. \tag{3}$$

On an f plane this further simplifies to the equation for topographic steering

$$\vec{v} \bullet \nabla H = 0. \tag{4}$$

For a homogenous fluid the geostrophic flow is given as

$$\vec{v} = \frac{g}{f}\vec{k} \times \nabla\zeta, \tag{5}$$

where g is the acceleration due to gravity. Combining these equations give

$$\frac{g}{f}\vec{k} \bullet \nabla\zeta \times \nabla H = 0. \tag{6}$$

This means that sea level slope (ζ) and the bottom depth (H) have parallel equiscalar surfaces, and in the case of topographic steering on a f plane

$$\zeta = \zeta(H). \tag{7}$$

Thus for stationary geostrophic flow with a free surface, the isolines of the surface and the depth contours will be parallel. Other studies suggest that this is in fact what is observed. In the Norwegian Atlantic Current the observations show that the mean currents follow the isobaths, the maximum current coincides with the steepest bottom slope, and the flow nearly vanishes where the bottom locally becomes flat [*Orvik et al.*, 2001]. Analytical considerations of this are included by *Walin et al.* [2004]. Based on the above it appears justified that to the lowest order, we can construct the current field over the slope by scaling the observed velocity profile by the depth gradient ($v(x, z) = v_{obs}(z) \cdot \nabla H(x)/\nabla H_{obs}$). Further, this is modified to account for the baroclinicity in the outer part of the slope (where the bottom velocity vanishes because of the flat bottom) by utilizing the thermal wind relation (Figure 12). Combined with the temperature and salinity fields (Figure 12), volume, heat and freshwater fluxes are calculated (Table 2). In the slope region, the total volume flux is estimated to be 1.3 Sv. However, the water mass is a mixture of Atlantic Water $S_{AW} = 35.0$ and Coastal Water $S_{CW} = 34.3$ at the entrance to the Barents Sea. When considering only the fraction that contains coastal water the transport is 0.6 Sv. The associated heat flux is 34 TW relative to the reference temperature of 0°C, and freshwater flux ranges from 4.5 to 12.2 mSv for reference salinities from 34.8 to 35.0, respectively.

[20] The second contribution comes from the baroclinic currents in the offshore region. Assuming no friction, geostrophic flow and hydrostatic conditions the thermal wind relation integrated vertically from a depth z = −h upward is given by

$$\int_{-h}^{z} \frac{\partial v}{\partial z} dz' = \frac{-g}{\rho_r f} \int_{-h}^{z} \frac{\partial \rho}{\partial z} dz', \tag{8}$$

where z is the vertical coordinate positive upward, the x axis is defined as normal to the coast, v is the along-coast velocity, g is the acceleration due to gravity, $\rho_r = 1027.5$ kg m^{-3} is the reference density, f is the Coriolis parameter, and ρ is the density. Integrating equation (8) over a cross section in the xz plane gives

$$\int_{-\infty}^{0}\int_{-h}^{0}\left[\int_{-h}^{z} \frac{\partial v}{\partial z} dz'\right] dzdx = \frac{-g}{\rho_r f}\int_{-\infty}^{0}\int_{-h}^{0}\left[\int_{-h}^{z} \frac{\partial \rho}{\partial x} dz'\right] dzdx. \tag{9}$$

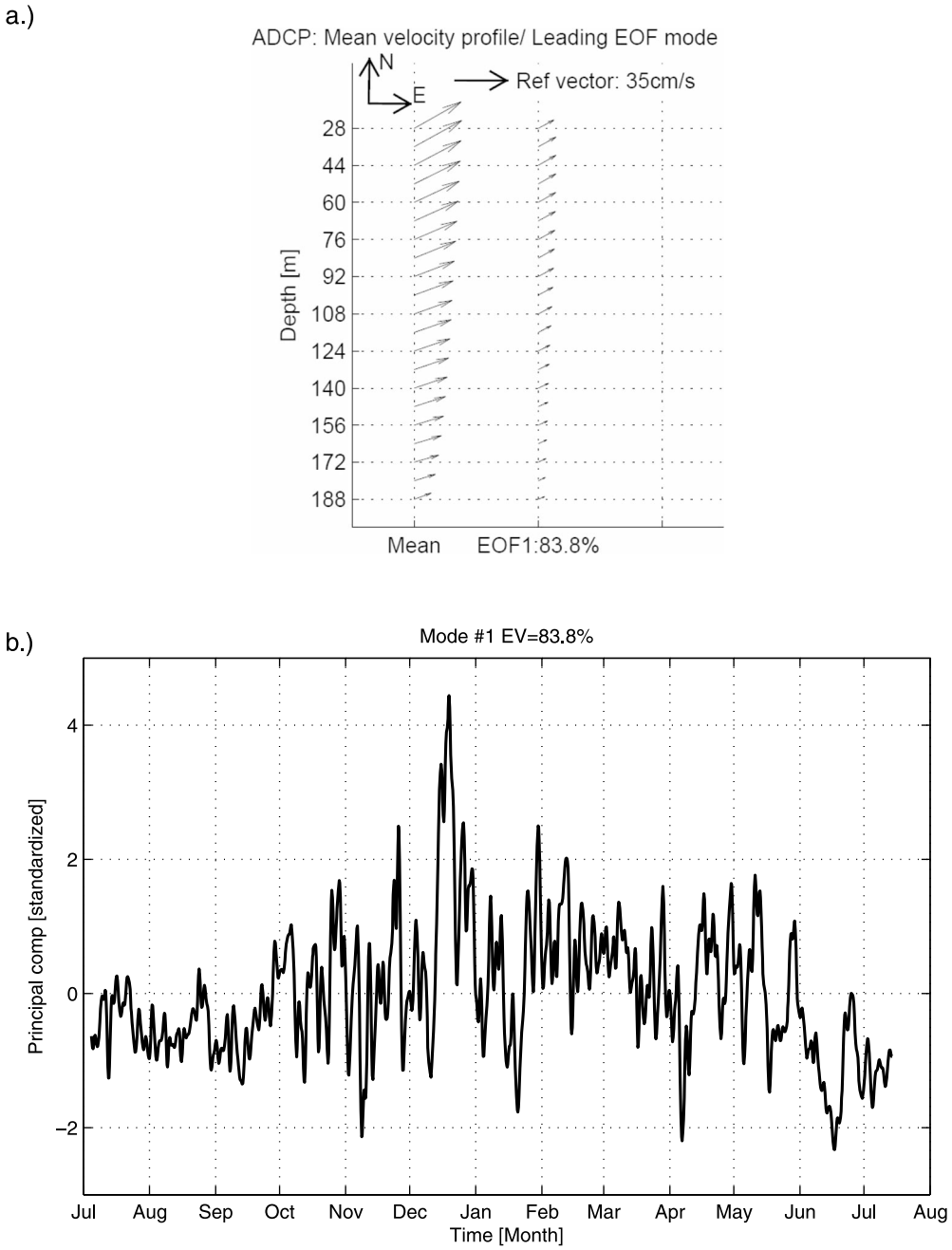

Figure 8. (a) The vertical profile of the mean current and the leading EOF modes of the ADCP data and (b) the associated principal components of the leading EOF modes. Prior to the EOF decomposition the data were low-pass filtered as described in Figure 6 and the mean velocity profile was removed.

Assuming that the density at the offshore boundary is homogeneous and equals $\rho(-h)$ (applies only to winter situation), the total transport can be estimated from single profiles at x = 0 (see Figure 11)

$$\mathrm{Vol} = \int_{-\infty}^{0}\int_{-h}^{0} v(z)\,dz\,dx = \frac{g}{\rho_r f}\int_{-h}^{0}\int_{-h}^{z}[\rho(-h) - \rho(z)]\,dz'\,dz, \tag{10}$$

with the velocity v(−h) = 0. From equation (10) the transport outside (seaward) can be calculated from single stations [*Jakhelln*, 1936], and this is applied to the repeated hydrographic profiles at the Ingøy fixed station. Again, the water mass is a mixture of Atlantic Water S_{AW} = 35.0 and Coastal Water S_{CW} = 34.3 at the entrance to the Barents Sea. Since the isohalines align parallel to the isopycnals (Figure 11) we can define the fraction of NCC water

$$\alpha(z) = \frac{S_{AW} - S(z)}{S_{AW} - S_{CW}}, \tag{11}$$

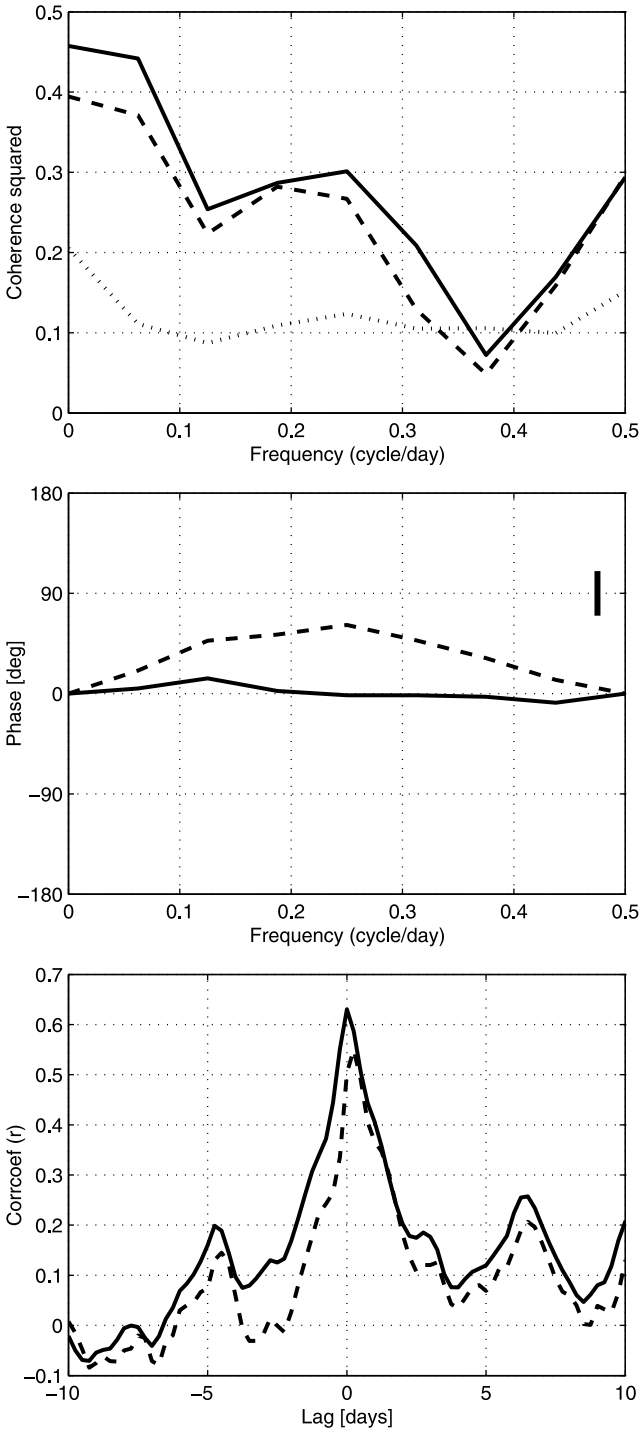

Figure 9. Relations between the principal component of the leading EOF mode at Ingøy and CTW model (solid) and along-coast wind (dashed) showing (top) coherence, (middle) phase, and (bottom) lagged correlation. The CTW is run for the Norwegian coast from (59.0°N, 4.5°E) to (70.8°N, 30°E) using the local along-coast wind stress as forcing. The output from the model is taken from the grid point representing Ingøy. Uncertainties are given in Figure 9a as dotted lines showing the 99% significance level, and in Figure 9b a thick bar represents the standard error.

where S(z) is the observed salinity profile. Combined with equation (10) the volume transport of the offshore branch is

$$\mathrm{Vol_{NCC}} = \int_{-\infty}^{0}\int_{-\mathrm{h}}^{0} \mathrm{v(z)}\alpha(\mathrm{z})\mathrm{dzdx} = \frac{\mathrm{g}}{\rho_{\mathrm{r}}\mathrm{f}}\int_{-\mathrm{h}}^{0}\int_{-\mathrm{h}}^{\mathrm{z}}[\rho(-\mathrm{h}) - \rho(z)]\alpha(\mathrm{z})\mathrm{dz'dz}. \quad (12)$$

The freshwater flux of the offshore branch relative to a reference salinity (S_{ref}) is then given by

$$FW_{NCC} = V(z)\beta(z), \quad (13a)$$

$$\beta(z) = \frac{S_{ref} - S(z)}{S_{ref}}. \quad (13b)$$

Combining equations (10) and (13)

$$\mathrm{FW_{NCC}} = \int_{-\infty}^{0}\int_{-\mathrm{h}}^{0} \mathrm{v(z)}\beta(\mathrm{z})\mathrm{dzdx} = \frac{\mathrm{g}}{\rho_{\mathrm{r}}\mathrm{f}}\int_{-\mathrm{h}}^{0}\int_{-\mathrm{h}}^{\mathrm{z}}[\rho(-\mathrm{h}) - \rho(\mathrm{z})]\beta(\mathrm{z})\mathrm{dz'dz}. \quad (14)$$

[21] The above expressions are for the baroclinic component of the Norwegian Coastal Current in a presumed geostrophic balance where a reference density interface corresponding to zero velocity outcrops to the surface [*Jakhelln*, 1936]. The hydrographic sections show that the σ_o = 27.6 kg m^{-3} interface, intercepts the slope at about the 300 m isobath, and indeed outcrops to the surface during winter (Figure 4). During summer this is not the case. At that time the Coastal Water extends farther northward and a density interface outcropping at the surface cannot readily be defined (Figure 5). Figure 11 shows the position of the repeated hydrographic station at Ingøy (X = 0) at the outer part of the slope. According to the discussion above regarding the slope current, the bottom velocity should be small in this part of the slope due to relatively flat bottom (Figure 12). Based on the above and CTD profiles obtained in the offshore region, it is justifiable to apply the single station method, to the repeated hydrographic profiles at Ingøy, when we restrict ourselves to winter (DJFM) months.

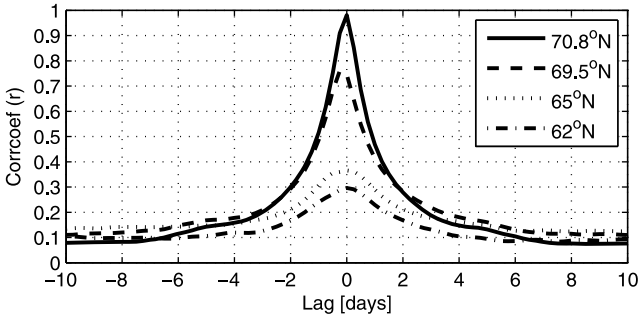

Figure 10. Lagged correlation between the local wind at Ingøy and other positions southwestward along the coast.

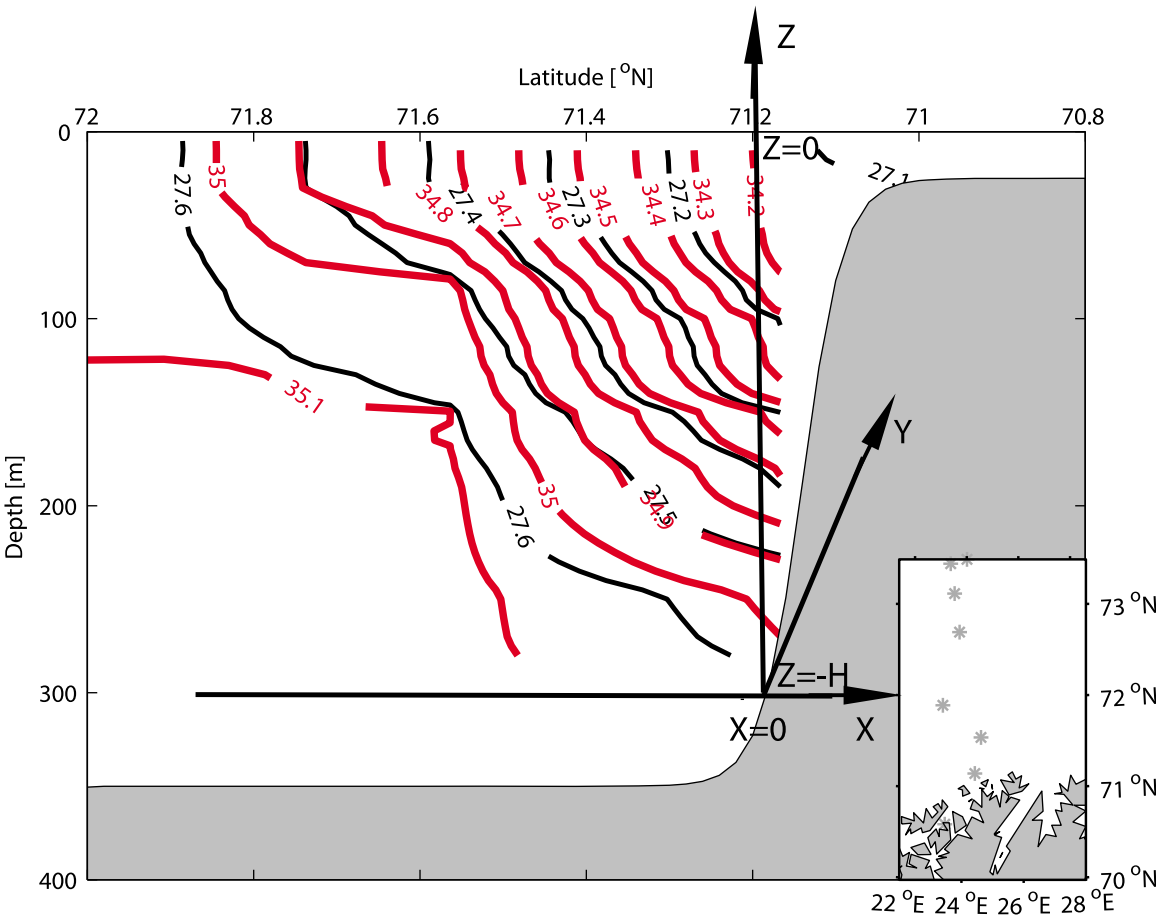

Figure 11. Schematic of a cross section normal to the coast at Ingøy. The *x* axis is defined positive normal toward the coast, and the *z* axis is defined positive upward. The hydrographic data used to construct the fields of salinity (red) and density (black) are the same as in Figure 4.

[22] The estimated fluxes are summarized in Table 2. Considering the different contributions the estimated total volume and freshwater fluxes of the NCC are 1.8 Sv and 41.2 mSv, respectively, relative to a reference salinity of 35.0. The largest contributions are from the offshore branch both for the volume and the freshwater flux. A robust estimate of the interannual to decadal variability in the freshwater content is

$$\mathrm{FW} = \int_{-300}^{0} \frac{\mathrm{S_{ref}} - \mathrm{S}}{\mathrm{S_{ref}}} \mathrm{dz}, \qquad (15)$$

where in this case we choose the reference salinity S_{ref} = 35.0 and S is the observed salinity at the Ingøy repeated station (Figure 13). The result from this shows that the freshwater content was relatively high in the 1930–1940s, the late 1960s and 1970s had small values, a subsequent period with high values in the 1980–1990s and reduced freshwater content up to present.

[23] The baroclinic method used for the offshore branch cannot be applied to the heat flux, since the assumption of the isotherms following the isopycnals is not valid in this region. Thus the heat flux estimate of 34 TW includes the slope branch only, but can nevertheless be regarded as a lower limit.

5. Discussion

[24] One main result of this study is that the volume flux of the NCC is 1.8 Sv, larger than those reported by *Björk et al.* [2001] and *Blindheim* [1989]. To assess if the differences are indeed, statistically significant, we need to obtain estimates of the uncertainties. In the slope current the main uncertainty is related to the estimated velocity field. This error is difficult to assess, but a assuming an uncertainty of the order 10% of the maximum current (about 0.03 ms^{-1}) would lead to a at maximum a 10% error in the volume flux, i.e., less than 0.1 Sv. In the baroclinc component the major uncertainty is the assumption of the zero bottom velocity, and further note that this uncertainty increases with the cross-sectional area. Dividing the estimated baroclinic transport (1.1 Sv) by its cross section (Width (~100 km)*Depth (~300 m) /2; dimensions are taken from Figure 4) we obtain a mean velocity of ~0.07 ms^{-1}. Based on the long-term mean values from the monitoring in the Barents Sea Opening reasonable estimates of the near bottom currents are of the order 0.01–0.03 ms^{-1} giving uncertainties of 0.15–0.45 Sv. Based

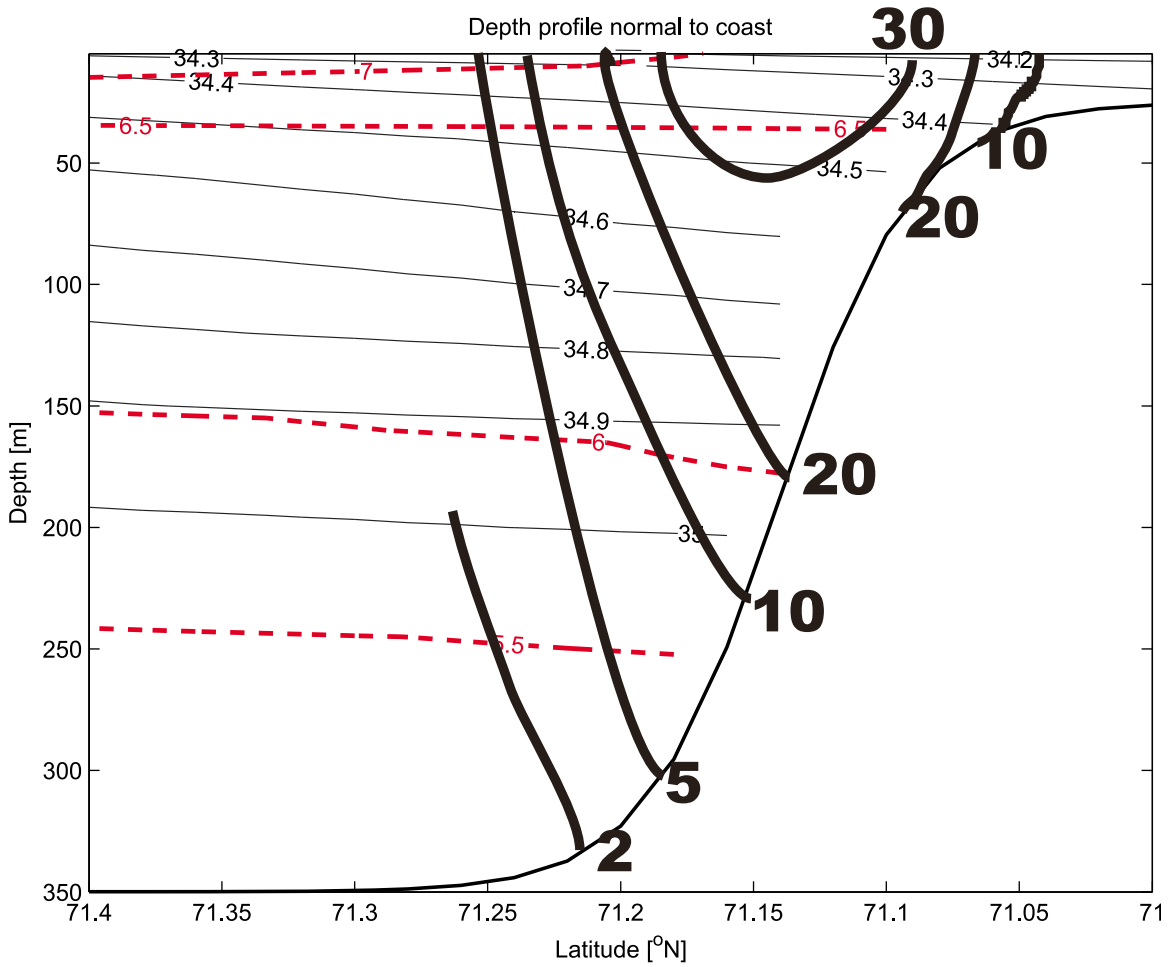

Figure 12. A section normal to the coast from Ingøy including the annual mean cross section velocities, i.e., along the slope (thick black), salinity (thin black), and temperature (dashed red).

on this, but acknowledging that the error is still not fully resolved, it appears fair to state that present estimates are significantly higher than those previously reported. Further, it should be noted that there was no discussion of the error in the previous studies.

[25] There are also points to be made regarding the contribution from the two different components of the NCC discussed here. First, the estimate of 0.8 SV based on the *Blindheim* [1989] data is limited to the nearshore component and corresponds reasonably well with the estimate of the slope current estimated in this study of 0.6 Sv. Second, *Björk et al.* [2001] estimated the baroclinic transports of the NCC for the upper 200 m to 0.7 Sv. This is close to the estimate of the offshore branch based on the single station method when integrating from 200 m to surface. However, since the baroclinic currents are still significant below 200 m (see Figure 12), we obtain an additional contribution when integrating from 300 m to the surface. As mentioned, the baroclinic estimates are from the winter months (DJFM). The estimate of *Björk et al.* [2001] was based on climatology whereas our estimate was based on winter data only. Considering the seasonality of the NCC, the freshwater loading is larger during the summer half year due to spring melt and fall precipitation, and that during winter the NCC extends deeper. In terms of the fluxes both these effects would tend to increase the transports. It is therefore difficult to conclude that the estimated winter estimates for the baroclinic currents are significantly different from the annual mean. *Dickson et al.* [2007] in their review of the freshwater fluxes in the Arctic and Subarctic seas reported the contribution from the NCC to be 16 mSv relative to a reference salinity of 35.2. Their estimate was based on the *Blindheim* [1989] data and thus covers the slope branch only. Using the same reference value for salinity, the estimated freshwater flux of the baroclinic branch is 36 mSv. Adding the con-

Table 2. Transport Estimates of the Norwegian Coastal Current[a]

		Offshore		
	Slope	Z_{int} = 200	Z_{int} = 300	Total
Volume (Sv)	1.3	0.6	1.3	2.6
Volume NCC (Sv)	0.6	0.5	1.1	1.8
Freshwater relative to reference salinity 34.8 (mSv)	4.5	10	21	26
Freshwater relative to reference salinity 35.0 (mSv)	12	14	29	41
Heat flux (TW)	34			

[a]For the slope branch the velocity field is the mean from July 2007 to July 2008. The offshore estimates are taken as the mean based on all (433) hydrographic profiles during the months (DJFM) to reduce the uncertainty.

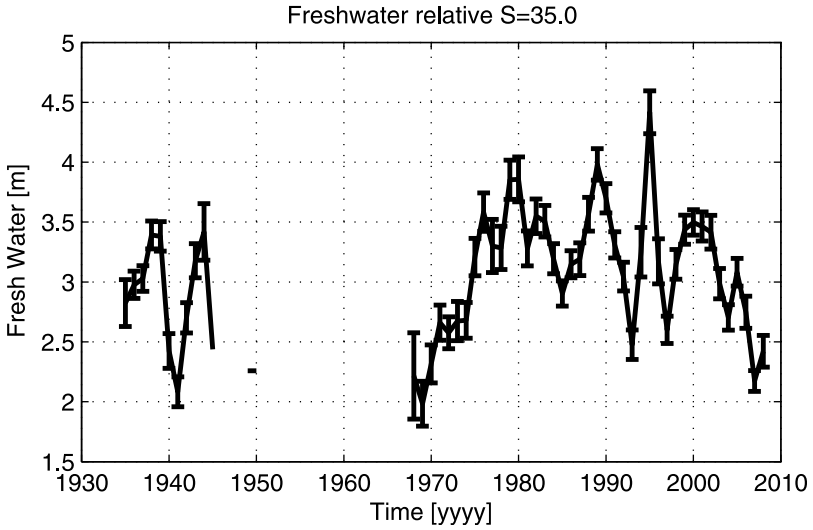

Figure 13. Freshwater transport for the baroclinic offshore branch calculated relative to a salinity S_{ref} = 35. The estimates are based on repeated hydrographic profiles from the Ingøy fixed station, about 300 m depth. The line is the 3 year mean and the bars indicate the associated standard deviation. Total number of stations is 1386 and the distribution between the months is rather uniform. Remarkably 110 profiles were occupied through World War II.

tribution from the slope branch, the total freshwater flux into the Barents Sea estimated in this study exceeds previous estimates by a factor of more than two. Compared to the total freshwater input to the Arctic of ~250 mSv relative to S = 34.8 [*Dickson et al.*, 2007] the estimated contribution herein of 26 mSv is only about 10% and should therefore not call for any revision of the Arctic freshwater budget. However, in volume budgets for the Arctic the larger volume fluxes of the NCC should be considered.

[26] The fate of the Norwegian Coastal Current is determined largely by the shelf-ocean exchange. According to *Huthnance et al.* [2009] the dominant effects controlling this exchange are wind forcing and ocean eddies, but they noted that there is no clear estimate of the eddy separation rate to the interior of the Norwegian Sea. Off northern Norway, between Lofoten (~13°E) and the Bear Island-Fugløya section (~20°E), *Gascard et al.* [2004] found a reduction in the radioactive tracer ^{129}I transported by the NCC of 35%. It could be questioned however if this reduction rate applies to the NCC as a whole due to the anomalous narrow shelf and steep slope in this region that cause anomalously large mixing by eddy separation to the ocean interior [*Köhl*, 2007]. In accordance with this view the observed salinity changes along the NCC in general indicate a smaller mean mixing rate than reported by *Gascard et al.* [2004].

[27] The distribution of the freshwater is intimately linked to the pathways entering the Barents Sea. Divergence of the NCC toward the North Cape Bank is suggested based on the drifter data (Figure 2), and in particular at depth (100 m) there is a marked eastward divergence in the salinity field (Figure 3). This is in accordance with topographic steering at the eastern rim and leads to dispersion of the NCC over the North Cape Bank itself.

[28] The results of the current meter data analysis point to the relatively strong role of the wind in the forcing of the NCC in the sense of CTW in the Barents Sea. The cross-spectral analysis (Figure 9) shows this relation for time scales from 3 to 16 days. However, the similar relation is probably valid also on the annual scale connected to anomalously strong southwesterly wind forcing and slope branch of the NCC during the fall and winter seasons (Figure 8a and Table 1). The increased vertical velocity shear during fall and winter (Table 1) is in accordance with anomalous downwelling-favorable winds and stronger CTW forcing during these seasons. However, the baroclinic field changes, e.g., when going from downwelling- to upwelling-favorable winds, and thus to separate the relative effect of the wind to buoyancy forcing is difficult.

[29] Understanding the relative roles of the buoyancy and wind forcing is a key to assess how a possible change in the wind and freshwater forcing under a future climate will project onto the NCC. As such, we propose that the variability of the NCC in the entrance to the Barents Sea can be separated into a partially wind-driven slope branch and an offshore branch driven principally by the buoyancy field. Even though it is beyond the scope of this work, this could be used to investigate effects on the recruitment of fish species such as cod and herring that spend their early life stage in the coastal regions, as well as effects on the climate variability in the Barents Sea. Looking ahead toward an anticipated global climate change, the effect on the NCC would critically depend on changes to the mean and seasonal cycle of both the freshwater and wind forcing.

6. Conclusions

[30] The mean and variability of transports by the Norwegian Coastal Current in the Barents Sea is investigated by a combination of current meter, hydrographic and wind data. The transports of the NCC can be divided into a partly barotropic slope branch, and an outer branch associated with the light NCC water that overlies the Atlantic water further offshore. The total transports of the NCC are estimated to 1.8 Sv for the volume flux, the freshwater flux is 26 mSv

relative to a reference salinity of 34.8, and the heat flux calculated for the slope branch only is 34 TW. These transports are generally higher than previous estimates by about 100%.

[31] The variability of the Norwegian Coastal Current is significantly coherent with the wind field and consistent with a continental shelf wave for periods of days to weeks. This indicates that the response at any location along the coast consist of a combination of direct forcing by the local wind and a propagating signal forced by the winds along the upstream portion of the coast. A similar mechanism could also explain the increased transport of the slope branch during fall and winter compared to spring and summer. In terms of what is driving the mean transports, the buoyancy is still the major forcing.

[32] The relatively simple topography at the Ingøy section makes this an ideal location for monitoring the Norwegian Coastal Current at the entrance to the Barents Sea and is located in the conveyor belt of juvenile fish larvae and oceanic transports of freshwater and heat toward the Arctic.

[33] **Acknowledgments.** This study was supported by the Norwegian Research Council projects NorClim, Pocahontas, and iAOOS. It is contribution A330 from the Bjerknes Centre for Climate Research. The authors would like to thank the reviewers for critical comments that helped to improve the paper.

References

Aagaard, K., L. K. Coachman, and E. C. Carmack (1981), On the halocline of the Arctic Ocean, *Deep Sea Res.*, *28*, 529–545, doi:10.1016/0198-0149(81)90115-1.

Aure, J., and Ø. Østensen (1993), Hydrographical normals and long-term variations in Norwegian coastal waters from 1936 to 1992, *Fisken Havet Rapp. 6*, 67 pp., Inst. of Mar. Res, Bergen, Norway.

Baliño, B. M. (1993), Nutrient inputs to the North Sea, Skagerrak and Kattegat: River concentrations and loads from 1980 to 1990, technical report, 69 pp., Høyteknologisenteret, Bergen, Norway.

Björk, G., B. G. Gustafsson, and A. Stigebrandt (2001), Upper layer circulation in the Nordic Seas as inferred from the spatial distribution of heat and freshwater content and potential energy, *Polar Res.*, *20*, 161–168, doi:10.1111/j.1751-8369.2001.tb00052.x.

Blindheim, J. (1989), Cascading of Barents Sea bottom water into the Norwegian Sea, *Rapp. P.-V. Reun. Cons. Int. Explor. Mer*, *188*, 49–58.

Bratseth, A. M. (1986), Statistical interpolation by means of successive corrections, *Tellus*, *38A*, 439–447, doi:10.1111/j.1600-0870.1986.tb00476.x.

Dickson, R. R., B. Rudels, S. Dye, M. Karcher, J. Meincke, and I. Yashayaev (2007), Current estimates of freshwater flux through Arctic and subarctic seas, *Prog. Oceanogr.*, *73*, 210–230, doi:10.1016/j.pocean.2006.12.003.

Eggvin, J. (1940), The movements of a cold water front, *Rep. Norw. Fish. Mar. Invest.*, *6*(5), 1–151.

Eggvin, J. (1946), The physical oceanography and our fisheries (in Norwegian), in *Forskning og Framsteg*, edited by C. L. Godske, pp. 68–89, J. W. Eide, Bergen, Norway.

Garvine, R. W. (1995), A dynamical system for classifying buoyant coastal discharges, *Cont. Shelf Res.*, *15*, 1585–1596, doi:10.1016/0278-4343(94)00065-U.

Gascard, J. C., G. Raisbeck, S. Sequeira, F. Yiou, and K. A. Mork (2004), The Norwegian Atlantic Current in the Lofoten basin inferred from hydrological and tracer data (129 I) and its interaction with the Norwegian Coastal Current, *Geophys. Res. Lett.*, *31*, L01308, doi:10.1029/2003GL018303.

Gill, A. E. (1982), *Atmosphere-Ocean Dynamics*, *Int. Geophys. Ser.*, vol. 30, Academic, San Diego, Calif.

Gill, A. E., and A. J. Clarke (1974), Wind-induced upwelling, coastal currents and sea-level changes, *Deep Sea Res.*, *21*, 325–345.

Gustafsson, B. (1997), Interaction between Baltic Sea and North Sea, *Ocean Dyn.*, *49*, 165–183, doi:10.1007/BF02764031.

Helland-Hansen, B., and F. Nansen (1909), The Norwegian Sea: Its physical oceanography based upon the Norwegian research 1900–1904, *Rep. Norw. Fish. Mar. Invest.*, *2*(2), 1–360.

Hjort, J., and H. H. Gran (1899), Currents and pelagic life in the northern ocean: Report on fishery and marine investigations 1895–1897, *Bergen Mus. Skr.*, *6*, 1–22.

Huthnance, J. M., J. T. Holt, and S. L. Wakelin (2009), Deep ocean exchange with west European shelf seas, *Ocean Sci.*, *5*, 621–634, doi:10.5194/os-5-621-2009.

Iden, K. A. (1997), Meteorologi–værforholdene på Norskekysten, in *Den Norske Los*, vol. I, pp. 129–146, Statens kartverk Sjøkartverket, Stavanger, Norway.

Jakhelln, A. (1936), The water transport of gradient currents, *Geofys. Publ.*, *XI*, 1–14.

Kaihatu, J. M., R. A. Handler, G. O. Marmorino, and L. K. Shay (1998), Empirical orthogonal function analysis of ocean surface currents using complex and real-vector methods, *J. Atmos. Oceanic Technol.*, *15*, 927–941, doi:10.1175/1520-0426(1998)015<0927:EOFAOO>2.0.CO;2.

Knudsen, M. (1899), De hydrografiske forhold i de Danske farvande indenfor Skagen i 1894–1898: Beretning fra kommisjonen for videnskabelige undersøgelser av de Danske farvande (in Danish), *Copenhagen*, *2*, 17–97.

Köhl, A. (2007), Generation and stability of a quasi-permanent vortex in the Lofoten basin, *J. Phys. Oceanogr.*, *37*, 2637–2651, doi:10.1175/2007JPO3694.1.

Martinsen, E. A. (1981), The barotropic current due to storm surges along the coast of Norway, in *The Norwegian Coastal Current, Proceedings of the Norwegian Coastal Current Symposium, Geilo, 9–12 September 1980*, edited by R. Sætre and M. Mork, pp. 500–517, Univ. of Bergen, Bergen, Norway.

Montgomery, R. B. (1974), Comments on "Seasonal variability of the Florida Current" by Niiler and Richardson, *J. Mar. Res.*, *32*, 533–534.

Oppenheim, A. V., and R. W. Schafer (1989), *Discrete-Time Signal Processing*, Prentice-Hall, New Jersey.

Orvik, K. A., Ø. Skagseth, and M. Mork (2001), Atlantic inflow to the Nordic Seas: Current structure and volume fluxes from moored current meters, VM-ADCP and SeaSoar-CTD observations, 1995–1999, *Deep Sea Res.*, *48*, 937–957, doi:10.1016/S0967-0637(00)00038-8.

Sætre, R. (1999), Features of the central Norwegian shelf circulation, *Cont. Shelf Res.*, *19*, 1809–1831, doi:10.1016/S0278-4343(99)00041-2.

Sætre, R. (Ed.) (2007), *The Norwegian Coastal Current—Oceanography and Climate*, Tapir Acad., Trondheim, Norway.

Sætre, R., and M. Mork (Eds.) (1981), *The Norwegian Coastal Current, Proceedings of the Norwegian Coastal Current Symposium, Geilo, 9–12 September 1980*, Univ. of Bergen, Bergen, Norway.

Sætre, R., J. Aure, and D. S. Danielssen (2003), Long-term hydrographic variability patterns off the Norwegian coast and in the Skagerrak, *ICES Mar. Sci. Symp.*, *219*, 150–159.

Schauer, U., A. Beszczynska-Moller, W. Walczowski, E. Fahrbach, J. Piechura, and E. Hansen (2008), Variation of measured heat flow through the Fram Strait between 1997 and 2006, in *Arctic-Subarctic Ocean Fluxes: Defining the Role of the Northern Seas in Climate*, edited by R. R. Dickson et al., pp. 65–85, Springer, Dordrecht, Netherlands.

Smedsrud, L. H., R. Ingvaldsen, J. E. Ø. Nilsen, and Ø. Skagseth (2010), Heat in the Barents Sea: Transport, storage, and surface fluxes, *Ocean Sci.*, *6*, 219–234, doi:10.5194/os-6-219-2010.

Tollan, A. (1976), River runoff in Norway, in *Freshwater on the Sea*, edited by S. Skreslett et al., pp. 11–13, Assoc. of Norw. Oceanogr., Oslo.

Vikebø, F., S. Sundby, B. Ådlandsvik, and Ø. Fiksen (2005), The combined effect of transport and temperature on distribution and growth of larvae and pelagic juveniles of Arcto-Norwegian cod, *ICES J. Mar. Sci.*, *62*, 1375–1386, doi:10.1016/j.icesjms.2005.05.017.

Walin, G., G. Brostrøm, J. Nilsson, and O. Dahl (2004), Baroclinic boundary currents with downstream decreasing buoyancy: A study of an idealized Nordic Seas system, *J. Mar. Res.*, *62*, 517–543, doi:10.1357/0022240041850048.

Whitney, M. M., and R. W. Garvine (2005), Wind influence on a coastal buoyant outflow, *J. Geophys. Res.*, *110*, C03014, doi:10.1029/2003JC002261.

K. F. Drinkwater and Ø. Skagseth, Institute of Marine Research, PO Box 1870, Nordnes, N-5817 Bergen, Norway. (oystein.skagseth@imr.no)

E. Terrile, Data Environment Analysis Modelling, 11 Via Della Casina, I-56017 Pisa, Italy.